STATISTICS, OPTIMIZATION AND INFORMATION COMPUTING
Stat., Optim. Inf. Comput., Vol. **10**, March 2022, pp 484–504.
Published online in International Academic Press (www.IAPress.org)

A New Compound Generalization of the Lomax Lifetime Model: Properties, Copulas and Modeling Real Data

Mohamed K. A. Refaie *

Agami High Institute of Administrative Sciences, Alexandria, Egypt

Abstract A new compound generalization of the Lomax lifetime model is presented and studied. The novel model is established based on the Poisson Topp-Leone family of Merovci et al. (2020). The novel density can be "right skewedwith heavy tail", "symmetric" and "left skewedwith heavy tail". The corresponding failure rate can be "monotonically decreasing", "increasingconstant", "upside down", "upside down-constant" and "reversed J-shape". Relevant characteristics are derived and discussed. numerical and graphical analysis for some statistical properties are presented. we derived some new bivariate extensions via some common copulas. Graphical assessment for the maximum likelihood estimation is presented. Graphical assessment for the maximum likelihood estimation is presented. Two real-life data sets are analyzed and modelled using the novel model. The new model proven its superiority against fourteen competitive Lomax extensions.

Key Words: Poisson Topp-Leone family; Lomax model; Maximum likelihood estimation; Farlie Gumbel Morgenstern; Clayton copula.

Mathematics Subject Classification: 60E05; 62G05; 62N05; 62P30.

DOI:10.19139/soic-2310-5070-1207

1. Introduction

The Lomax or Pareto type II distribution (Lomax [30]), is a heavy-tail probabilistic model used in modeling business, actuarial science, biological sciences, engineering, economics, income and wealth inequality, queueing theory, size of cities and Internet traffic data sets. Harris [24] and Atkinson and Harrison [9] employed the Lomax (Lx) distribution in modeling data obtained from income and wealth. Corbellini et al. [17] used the Lx distribution firm size data modeling. For applications in reliability and life testing experiments see Hassan and Al-Ghamdi [25]. The Lx model is known as a special distribution form of Pearson system (type VI) and has also considered as a mixture of standard exponential (Exp) and standard gamma (Ga) distributions. The Lx model belongs to the family of "monotonically decreasing" hazard rate function (HRF) and considered as a limiting model of residual lifetimes at great age (see Balkema and de Hann [10] and Chahkandi and Ganjali [12]). The Lx distribution has been suggested as heavy tailed alternative model to the standard Exp, standard Weibull (W) and standard Gam distributions (see Bryson [11]). For details about relation between the Lx model and the Burr XII and Compound Gamma (CGam) models see Tadikamalla [51] and Durbey [15]. A random variable (rv) Y has the Lomax (Lx) distribution with two parameters ζ_1 and ζ_2 if it has cumulative distribution function (CDF) (for $Y > 0$) given by

$$G_{\zeta_1,\zeta_2}(y) = 1 - \left(1 + \frac{y}{\zeta_2}\right)^{-\zeta_1}, \tag{1}$$

*Correspondence to: Mohamed K. A. Refaie (refaie_top@yahoo.com).Agami High Institute of Administrative Sciences, Alexandria, Egypt.

ISSN 2310-5070 (online) ISSN 2311-004X (print)

where $\zeta_1 > 0$ and $\zeta_2 > 0$ are the shape and scale parameters, respectively. Then the corresponding probability density function (PDF) of (1) is

$$\mathbf{g}_{\zeta_1,\zeta_2}(y) = \frac{\zeta_1}{\zeta_2}\left(1+\frac{y}{\zeta_2}\right)^{-(\zeta_1+1)}.$$

The main aim of this work is to provide a flexible extension of the Lx distribution using the Poisson Topp-Leone-G (PTL-G) family defined by Merovci et al. [43]. The CDF of the PTL-G family can be expressed as

$$F_{a,b}(y) = \frac{1}{b_*}\left(1-\exp\left\{-bG_{\underline{\phi}}(y)^a\left[2-G_{\underline{\phi}}(y)\right]^a\right\}\right)|_{y\in\mathbb{R}}, \tag{2}$$

where $b_* = 1-\exp(-b)$ and $a, b > 0$. The corresponding PDF can be written as

$$f_{a,b}(y) = 2ba\frac{\mathbf{g}_{\underline{\phi}}(y)\,G_{\underline{\phi}}(y)^{a-1}\,\overline{G}_{\underline{\phi}}(y)\left[2-G_{\underline{\phi}}(y)\right]^{a-1}}{b_*\exp\left\{bG_{\underline{\phi}}(y)^a\left[2-G_{\underline{\phi}}(y)\right]^a\right\}},$$

where $\overline{G}_{\underline{\phi}}(y) = 1-G_{\underline{\phi}}(y)$ refers to the reliability function of the baseline model. The CDF of the Poisson Topp-Leone Lomax (PTL-Lx) can then be derived as

$$F_{\underline{\Theta}}(y) = \frac{1}{b_*}\left(1-\exp\left\{-b\left[1-\left(1+\frac{y}{\zeta_2}\right)^{-2\zeta_1}\right]^a\right\}\right)|_{y\in\mathbb{R}}, \tag{3}$$

The corresponding PDF can be written as

$$f_{\underline{\Theta}}(y) = 2\frac{ba\zeta_1}{\zeta_2 b_*}\frac{\left(1+\frac{y}{\zeta_2}\right)^{-2\zeta_1-1}\left[1-\left(1+\frac{y}{\zeta_2}\right)^{-2\zeta_1}\right]^{a-1}}{\exp\left\{b\left[1-\left(1+\frac{y}{\zeta_2}\right)^{-2\zeta_1}\right]^a\right\}}. \tag{4}$$

Due to Merovci et al. [43], the PDF of the PTL-Lx model in (3) can be expressed as

$$f_{\underline{\Theta}}(y) = \sum_{l,\kappa=0}^{\infty}\left[\varsigma_{l,\kappa}^{[1]}\,h_{a(l,\kappa)}(y) - \varsigma_{l,\kappa}^{[2]}\,h_{1+a(l,\kappa)}(y)\right], \tag{5}$$

where $h_\gamma(y) = \gamma\mathbf{g}_{\underline{\phi}}(y)\,G_{\underline{\phi}}(y)^{\gamma-1}$refers to the PDF of the exp-Lx model,

$$\varsigma_{l,\kappa}^{[1]} = \frac{ab^{l+1}(-1)^{l+\kappa}}{l!b_*a(l,\kappa)}\left(\frac{1}{2}\right)^{\kappa-a(l+1)}\binom{a(l+1)-1}{\kappa}$$

and

$$\varsigma_{l,\kappa}^{[2]} = \frac{ab^{l+1}(-1)^{l+\kappa}}{l!b_*(1+a(l,\kappa))}\left(\frac{1}{2}\right)^{\kappa-a(l+1)}\binom{a(l+1)-1}{\kappa}.$$

Equation (9) reveals that the density of Y can be expressed as a linear representation of exp-Lx density. So, several mathematical properties of the new family can be obtained by knowing those of the exp-Lx distribution. The CDF of the PTL-Lx model can also be expressed as a mixture of exp-Lx densities. By integrating (5), we obtain the same mixture representation

$$F_{\underline{\Theta}}(y) = \sum_{l,\kappa=0}^{\infty}\left[\varsigma_{l,\kappa}^{[1]}\,H_{a(l,\kappa)}(y) - \varsigma_{l,\kappa}^{[2]}\,H_{1+a(l,\kappa)}(y)\right] \tag{6}$$

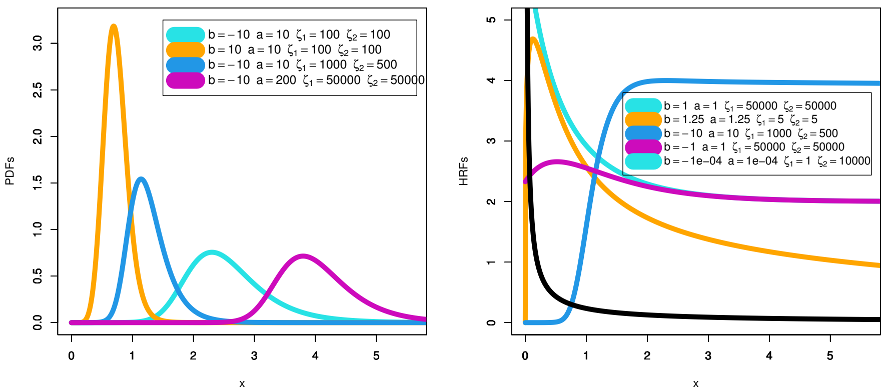

Figure 1. PDF and HRF plots for some selected parameters value.

where $a\,(l,\kappa) = a\,(l+1) + \kappa$ and $H_{a(l,\kappa)}(y)$ refers to the CDF of the exp-Lx model with power parameter $(a\,(l,\kappa) > 0)$. Many useful Lx extensions can be found in Gupta et al. [16] (the exponentiated Lomax model), Lemonte and Cordeiro [29] (Kumaraswamy Lomax, Macdonald Lomax and Beta Lomax models), Cordeiro et al. [18] (Gamma Lomax), Tahir et al. [53] (Weibull Lomax distribution), Yousof et al. [58] (transmuted Topp-Leone Lomax and reduced transmuted Topp-Leone Lomax), Cordeiro et al. (2018) (the one parameter Lomax system of densities), Altun et al. [6] (odd log-logistic Lomax, proportional reversed hazard rate Lomax and reduced odd log-logistic Lomax), Altun et al. [7] (Zografos-Balakrishnan Lomax distribution), Yousof et al.[59] (reduced Burr-Hatke Lomax), Elbiely and Yousof [19] (Weibull generalized Lomax, Rayleigh generalized Lomax and exponential generalized Lomax distributions), Yousof et al. [54]) (Topp Leone Poisson Lomax distribution), Goual and Yousof [33] (Lomax inverse Rayleigh), Gad et al. [31] (Burr XII Lomax, Lomax Burr XII and Lomax Lomax distributions), Chesneau and Yousof [13] (special generalized mixture Lomax), Yadav et al. [52] (Topp Leone Lomax distribution), and Ibrahim and Yousof [27] (Poisson Burr X generalized Lomax and Poisson Rayleigh generalized Lomax distributions). To illustrate the flexibility of the new PDF and its corresponding HRF we present Figure 1. Figure 1(left plot) gives some PDF plots for some selected parameters value. Figure 1(right plot) gives some HRF plots for some selected parameters value. Based on 1(left plot) the PTL-Lx density can be “right skewed”, “symmetric” and “left skewed”. Based on Figure 1(right plot) the PTL-Lx HRF can be “monotonically decreasing”, “increasing-constant”, “upside down”, “upside down-constant” and “reversed J-shape”.

The PTL-Lx model could be useful in modeling the asymmetric monotonically increasing hazard rate real data sets as illustrated in Figure 10, the real data sets which have no extreme observations as shown Figure 8, the real data sets which their Kernel density is semi-symmetric and bimodal as shown in Figure 11. The PTL-Lx model proved its wide applicability in modeling against common variable Lomax extensions. In modeling of the failure times of 84 aircraft windshields, the PTL-Lx model is compared with many well-known Lomax extensions such as the exponentiated Lomax extension, the odd log-logistic Lomax extension, the transmuted Topp-Leone Lx extension, the Kumaraswamy Lx extension, Gamma Lx extension, special generalized mixture Lx extension, the Burr Hatke Lx extension and the proportional reversed hazard rate Lx extension under the consistent-information criteria, Akaike information criteria, Bayesian information criteria and Hannan-Quinn information criteria. In statistical modeling of the service times of 63 aircraft windshields, the PTL-Lx model is compared with many well-known Lomax extensions such as the exponentiated Lomax extension, the odd log-logistic Lomax extension, the transmuted Topp-Leone Lx extension, the Kumaraswamy Lx extension, Gamma Lx extension, special generalized mixture Lx extension, the Burr Hatke Lx extension and the proportional reversed hazard rate Lx extension under the consistent-information criteria, Akaike information criteria, Bayesian information criteria and Hannan-Quinn information criteria. Additionally, we derived some new bivariate PTL-Lx (BPTL-Lx) via Farlie

Gumbel Morgenstern (FGM) copula, modified Farlie Gumbel Morgenstern (FGM) copula, Renyi's entropy and Clayton copula. The Multivariate PTL-Lx (MPTL-Lx) type is also presented using the Clayton copula. However, future works could be allocated to study these new models.

2. Mathematical properties

2.1. Moments, incomplete moments and generating function

The r^{th} ordinary moment of Y is given by

$$\mu'_{r,Y} = E(Y^r) = \int_{-\infty}^{\infty} y^r\, f\,(y)\, dy.$$

Then we obtain

$$\mu'_{r,Y} = \sum_{l,\kappa=0}^{\infty} \left[\varsigma_{l,\kappa}^{[1]}\, E(Z^r_{a(l,\kappa)}) - \varsigma_{l,\kappa}^{[2]}\, E(Z^r_{1+a(l,\kappa)}) \right]. \tag{7}$$

Henceforth, $Z_{a(l,\kappa)}$ denotes the exp-Lx distribution with power parameter$a\,(l,\kappa) > 0$.

$$\mu'_{r,Y} = \sum_{l,\kappa=0}^{\infty} \sum_{\hbar=0}^{r} \left[\begin{array}{c} \varsigma_{l,\kappa}^{[1]}\, \boldsymbol{\Delta}_{\hbar}^{(a(l,\kappa),r)} \mathcal{B}\left(a\,(l,\kappa)\,, 1 + \frac{\hbar - r}{\zeta_1}\right) \\ -\varsigma_{l,\kappa}^{[2]}\, \boldsymbol{\Delta}_{\hbar}^{(1+a(l,\kappa),r)} \mathcal{B}\left(1 + a\,(l,\kappa)\,, 1 + \frac{\hbar - r}{\zeta_1}\right) \end{array} \right] |_{(\zeta_1 > r)}.$$

where

$$\boldsymbol{\Delta}_{\hbar}^{(\gamma,r)} = \gamma \zeta_2^r\,(-1)^{\hbar} \binom{r}{\hbar}$$

and

$$\mathcal{B}(\tau_1, \tau_2) = \int_0^1 s^{\tau_1 - 1}\,(1-s)^{\tau_2 - 1}\, ds.$$

Setting $r = 1$ in (11), we have the mean of Y. The last integration can be computed numerically for most parent distributions. The skewness and kurtosis measures can be calculated from the ordinary moments using well-known relationships. The n^{th} central moment of Y, say $M_{n,Y}$, follows as

$$M_{n,Y} = E(y-\mu)^n = \sum_{\hbar=0}^{n} (-1)^h \binom{n}{h} (\mu'_1)^n\, \mu'_{n-h}.$$

The main applications of the first incomplete moment refer to the mean deviations and the Bonferroni and Lorenz curves. These curves are very useful in economics, reliability, demography, insurance and medicine. The d^{th} incomplete moment, say $\mathbf{I}_{d,Y}\,(t)$, of Y can be expressed from (9) as

$$\mathbf{I}_{d,Y}\,(t) = \int_{-\infty}^{t} y^d f\,(y)\, dy.$$

Then

$$\mathbf{I}_{d,Y}\,(t) = \sum_{l,\kappa=0}^{\infty} \sum_{\hbar=0}^{d} \left[\begin{array}{c} \varsigma_{l,\kappa}^{[1]} \boldsymbol{\Delta}_{\hbar}^{(a(l,\kappa),d)} \mathcal{B}_t\left(a\,(l,\kappa)\,, 1 + \frac{\hbar - d}{\zeta_1}\right) \\ -\varsigma_{l,\kappa}^{[2]}\, \boldsymbol{\Delta}_{\hbar}^{(1+a(l,\kappa),d)} \mathcal{B}_t\left(1 + a\,(l,\kappa)\,, 1 + \frac{\hbar - d}{\zeta_1}\right) \end{array} \right] |_{(\zeta_1 > d)}, \tag{8}$$

where

$$\mathcal{B}_u(\tau_1, \tau_2) = \int_0^u w^{\tau_1 - 1}\,(1-w)^{\tau_2 - 1}\, dw.$$

The mean deviations about the mean $[\delta_{1,Y} = E(|Y - \mu_1'|)]$ and about the median $[\delta_{2,Y} = E(|Y - M|)]$ of Y are given by $\delta_{1,Y} = 2\mu_{1,Y}' F(\mu_{1,Y}') - 2\mathbf{I}_{1,Y}(\mu_{1,Y}')$ and $\delta_{2,Y} = \mu_{1,Y}' - 2\mathbf{I}_{1,Y}(M)$, respectively, where $\mu_{1,Y}' = E(Y)$, M =Median$(y) = Q\left(\frac{1}{2}\right)$ is the median, $F(\mu_{1,Y}')$ is easily calculated from (3) and $\mathbf{I}_{1,Y}(t)$ is the first incomplete moment given by (8) with $d = 1$. Ageneral equation for $\mathbf{I}_{1,Y}(t)$ can be derived from (8) as

$$\mathbf{I}_{1,Y}(t) = \sum_{l,\kappa=0}^{\infty} \sum_{\hbar=0}^{1} \left[\begin{array}{c} \varsigma_{l,\kappa}^{[1]} \mathbf{\Delta}_{\hbar}^{(a(l,\kappa),1)} \mathcal{B}_t\left(a(l,\kappa), 1 + \frac{\hbar-1}{\zeta_1}\right) \\ -\varsigma_{l,\kappa}^{[2]} \mathbf{\Delta}_{\hbar}^{(1+a(l,\kappa),1)} \mathcal{B}_t\left(1 + a(l,\kappa), 1 + \frac{\hbar-1}{\zeta_1}\right) \end{array} \right] |_{(\zeta_1>1)},$$

The moment generating function (MGF) $M_Y(t) = E\left(e^{tY}\right)$ of Y can be derived from equation (5) as

$$M_Y(t) = \sum_{l,\kappa,r=0}^{\infty} \sum_{\hbar=0}^{r} \frac{t^r}{r!} \left[\begin{array}{c} \varsigma_{l,\kappa}^{[1]} \mathbf{\Delta}_{\hbar}^{(a(l,\kappa),r)} \mathcal{B}\left(a(l,\kappa), 1 + \frac{\hbar-r}{\zeta_1}\right) \\ -\varsigma_{l,\kappa}^{[2]} \mathbf{\Delta}_{\hbar}^{(1+a(l,\kappa),r)} \mathcal{B}\left(1 + a(l,\kappa), 1 + \frac{\hbar-r}{\zeta_1}\right) \end{array} \right] |_{(\zeta_1>r)},$$

By analyzing the μ_1', μ_2, skewness (β_1), kurtosis (β_2) and dispersion index (IxDis(Y)) numerically in Table 1, it is noted that, the β_1 of the PTL-Lx distribution can be positive. The spread for the β_2 of the PTL-Lx model is ranging from -361.2494 to ∞. The IxDis(Y) for the PTL-Lx model can be in $(0, 1)$ and also > 1 so it may be used as an "under-dispersed" and "over-dispersed" model.

Table 1: μ_1', μ_2, β_1, β_2 and IxDis(Y) of the PTL-Lx model.

b	a	ζ_1	ζ_2	μ_1'	μ_2	β_1	β_2	IxDis(Y)
-200	15	1000	1000	4.364728	0.117768	38.81793	-361.2494	0.026982
-100				4.034451	0.059426	117.5225	-1478.971	0.014729
-5				1.98×10^{-05}	6.733262	1.070338	1.243717	340223.1
-1				6.22×10^{-06}	4.287837	1.106353	1.38395	689418.0
1				2.29×10^{-06}	2.48×10^{-05}	∞	∞	10.85709
1	0.001	2	2	3.46×10^{-05}	0.00101	147.2431	215068.6	30.56841
	0.1			0.08937321	0.09784	15.69555	2500.37	1.094691
	1			0.7153228	0.51387	9.746332	867.1376	0.718369
	5			1.84746	0.87187	16.60932	1414.631	0.471928
	20			3.225945	1.80607	16.64470	1245.859	0.559861
	50			4.404508	3.31518	13.36668	890.0193	0.752678
	150			6.219562	6.78740	10.31248	607.2698	1.091299
	500			8.89245	14.1094	8.371584	442.6783	1.586673
	1000			10.85174	21.0158	7.685889	385.4050	1.936633
2.5	5	0.001	2.5	2.57×10^{-05}	0.1562103	18115.52	∞	6077.279
		0.1		1607.577	4925510	1.870781	5.826488	3063.933
		0.25		288.6213	733405.6	6.458681	52.3623	2541.066
		0.5		30.41014	28188.14	29.69571	1175.791	926.9325
		0.75		9.450391	1234.114	101.3404	17330.13	130.5887
		1		5.205106	81.08433	188.7926	105717.9	15.57784
-1	1	100	500	4.431624	3.112067	7.716443	20.5981	0.7022408
			1000	8.863248	12.44827	7.716443	20.5981	1.404482
			5000	44.31624	311.2067	7.716443	20.5981	7.022408
			10000	88.63248	1244.827	7.716443	20.5981	14.04482

2.2. Probability weighted moments

The PWMs are expectations of certain functions of a random variable and they can be defined for any random variable whose ordinary moments exist. The PWM method can generally be used for estimating parameters of a distribution whose inverse form cannot be expressed explicitly. The (d,r)th PWM of Y following the PTL-G family, say $\rho_{d,r}$, is formally defined by

$$\rho_{d,r} = E\left\{Y^d\, F(y)^r\right\} = \int_{-\infty}^{\infty} y^d\, F(y)^r\, f\left(y\right)\, dy.$$

Using equations (5) and (6), we can write

$$f_{\underline{\Theta}}\left(y\right)\, F_{\underline{\Theta}}(y)^r = \sum_{l,\kappa=0}^{\infty}\left[\nu_{l,\kappa}^{[1]}\, h_{a(l,\kappa)}(y) - \nu_{l,\kappa}^{[2]}\, h_{1+a(l,\kappa)}(y)\right],$$

where

$$\nu_{l,\kappa}^{[1]} = \sum_{\kappa=0}^{\infty}\frac{ab^{l+1}\left(-1\right)^{l+\kappa+\kappa}\left(\kappa+1\right)^l}{l!b_*^{r+1}a\left(l,\kappa\right)}\left(\frac{1}{2}\right)^{\kappa-a(l+1)}\binom{r}{\kappa}\binom{a\left(l+1\right)-1}{\kappa}$$

and

$$\nu_{l,\kappa}^{[2]} = \sum_{\kappa=0}^{\infty}\frac{ab^{l+1}\left(-1\right)^{l+\kappa+\kappa}\left(\kappa+1\right)^l}{l!b_*^{r+1}\left[1+a\left(l,\kappa\right)\right]}\left(\frac{1}{2}\right)^{\kappa-a(l+1)}\binom{r}{\kappa}\binom{a\left(l+1\right)-1}{\kappa}.$$

Then, the (d,r)th PWM of Y can be expressed as

$$\rho_{d,r} = \sum_{l,\kappa=0}^{\infty}\sum_{\hbar=0}^{d}\left[\begin{array}{c}\nu_{l,\kappa}^{[1]}\boldsymbol{\Delta}_{\hbar}^{(a(l,\kappa),d)}\mathcal{B}\left(a\left(l,\kappa\right),1+\frac{\hbar-d}{\zeta_1}\right)\\ -\nu_{l,\kappa}^{[2]}\,\boldsymbol{\Delta}_{\hbar}^{(1+a(l,\kappa),d)}\mathcal{B}\left(1+a\left(l,\kappa\right),1+\frac{\hbar-d}{\zeta_1}\right)\end{array}\right]|_{(\zeta_1>d)}\ .$$

2.3. Residual life and reversed residual life functions

The n^{th} moment of the residual life, say

$$m_{n,Y}(t) = E[(Y-t)^n \mid y>t],\ n=1,2,\ldots,$$

The n^{th} moment of the residual life of Y is given by

$$m_{n,Y}(t) = \frac{1}{1-F(t)}\int_t^{\infty}(y-t)^n dF_{\underline{\Theta}}(y).$$

Therefore,

$$m_{n,Y}(t) = \frac{1}{1-F_{\underline{\Theta}}(t)}\sum_{l,\kappa=0}^{\infty}\sum_{r=0}^{n}\sum_{\hbar=0}^{n}c_r^{[1]}\left\{\begin{array}{c}\varsigma_{l,\kappa}^{[1]}\,\boldsymbol{\Delta}_{\hbar}^{(a(l,\kappa),n)}\left[\begin{array}{c}\mathcal{B}\left(a\left(l,\kappa\right),1+\frac{\hbar-n}{\zeta_1}\right)\\ -\mathcal{B}_t\left(a\left(l,\kappa\right),1+\frac{\hbar-n}{\zeta_1}\right)\end{array}\right]\\ -\varsigma_{l,\kappa}^{[2]}\boldsymbol{\Delta}_{\hbar}^{(1+a(l,\kappa),n)}\left[\begin{array}{c}\mathcal{B}\left(1+a\left(l,\kappa\right),1+\frac{\hbar-n}{\zeta_1}\right)\\ -\mathcal{B}_t\left(1+a\left(l,\kappa\right),1+\frac{\hbar-n}{\zeta_1}\right)\end{array}\right]\end{array}\right\}|_{(\zeta_1>n)},$$

where $c_r^{[1]} = \binom{n}{r}\left(-t\right)^{n-r}$. Another interesting function is the mean residual life (MRL) function or the life expectation at age t defined by $m_1(t) = E\left[(y-t)\mid y>t\right]$, which represents the expected additional life length for a unit which is alive at age t. The MRL of Y can be obtained by setting $n=1$ in the last equation. The n^{th} moment of the reversed residual life, say $M_{n,Y}(t) = E\left[(t-Y)^n \mid y\leq t\right]$ for $t>0$ and $n=1,2,\ldots$ uniquely determines $F(y)$. We obtain

$$M_{n,Y}(t)=\frac{1}{F(t)}\int_0^t (t-y)^n dF(y).$$

Then, the n^{th} moment of the reversed residual life of Y becomes

$$M_{n,Y}(t)=\frac{1}{F_{\underline{\Theta}}(t)}\sum_{l,\kappa=0}^{\infty}\sum_{r=0}^{n}\sum_{\hbar=0}^{n}c_r^{[2]}\left[\begin{array}{c}\varsigma_{l,\kappa}^{[1]}\,\mathbf{\Delta}_{\hbar}^{(a(l,\kappa),n)}\mathcal{B}_t\left(a\left(l,\kappa\right),1+\frac{\hbar-n}{\zeta_1}\right)\\ -\varsigma_{l,\kappa}^{[2]}\mathbf{\Delta}_{\hbar}^{(1+a(l,\kappa),n)}\mathcal{B}_t\left(1+a\left(l,\kappa\right),1+\frac{\hbar-n}{\zeta_1}\right)\end{array}\right]|_{(\zeta_1>n)},$$

where $c_r^{[2]}=(-1)^r\binom{n}{r}t^{n-r}$. The mean inactivity time (MIT) or mean waiting time (MWT) also called the mean reversed residual life function is given by $M_{1,Y}(t)=E[(t-Y)\mid y\leq t]$, and it represents the waiting time elapsed since the failure of an item on condition that this failure had occurred in $(0,t)$.The MIT of the PTL-Lx distributions can be obtained easily by setting $n=1$ in the above equation.

2.4. Order statistics

Order statistics make their appearance in many areas of statistical theory and practice. Let $Y_1,Y_2,\ldots,Y_n$ be a random sample from the PTL-G family of distributions and let $Y_{(1:n)},Y_{(2:n)},\ldots,Y_{(n::n)}$ be the corresponding order statistics. The PDF of lth order statistic, say $Y_{l:n}$, can be written as

$$f_{l:n}\left(y\right)=\frac{f\left(y\right)}{\mathrm{B}\left(l,n-l+1\right)}\sum_{\kappa=0}^{n-l}\left(-1\right)^{\kappa}\binom{n-l}{\kappa}F\left(y\right)^{\kappa+l-1},\tag{9}$$

where $B(\cdot,\cdot)$ is the beta function. Substituting (3) and (4) in equation (9) and using a power series expansion,we get

$$f_{\underline{\Theta}}\left(y\right)\,F_{\underline{\Theta}}(y)^{\kappa+l-1}=\sum_{w_1,w_2=0}^{\infty}\left[\zeta_{l,\kappa}^{[1]}\,h_{a(w_1,w_2)}(y)-\zeta_{l,\kappa}^{[2]}\,h_{1+a(w_1,w_2)}(y)\right],$$

where

$$\zeta_{l,\kappa}^{[1]}=\sum_{\kappa=0}^{\infty}\frac{ab^{w_1+1}\left(-1\right)^{w_1+w_2+\kappa}\left(\kappa+1\right)^{w_1}}{w_1!b_*^{\kappa+l}\left[a\left(w_1,w_2\right)\right]}\left(\frac{1}{2}\right)^{w_2-a(w_1+1)}\binom{\kappa+l-1}{\kappa}\binom{a\left(w_1+1\right)-1}{w_2}$$

and

$$\zeta_{l,\kappa}^{[2]}=\sum_{\kappa=0}^{\infty}\frac{ab^{w_1+1}\left(-1\right)^{w_1+w_2+\kappa}\left(\kappa+1\right)^{w_1}}{w_1!b_*^{\kappa+l}\left[1+a\left(w_1,w_2\right)\right]}\left(\frac{1}{2}\right)^{w_2-a(w_1+1)}\binom{\kappa+l-1}{\kappa}\binom{a\left(w_1+1\right)-1}{w_2}.$$

The PDF of $Y_{l:n}$ can be expressed as

$$f_{l:n}\left(y\right)=\sum_{\kappa=0}^{n-l}\sum_{w_1,w_2=0}^{\infty}c_{\kappa}\left[\zeta_{l,\kappa}^{[1]}\,h_{a(w_1,w_2)}(y)-\zeta_{l,\kappa}^{[2]}\,h_{1+a(w_1,w_2)}(y)\right],$$

where

$$c_{\kappa}=\frac{1}{\mathrm{B}\left(l,n-l+1\right)}\left(-1\right)^{\kappa}\binom{n-l}{\kappa}.$$

Then, the density function of the PTL order statistics is a mixture of exp-Lx densities. The moments of $Y_{l:n}$ can be expressed as

$$E\left(Y_{l:n}^q\right)=\sum_{\kappa=0}^{n-l}\sum_{w_1,w_2=0}^{\infty}\sum_{\hbar=0}^{q}c_{\kappa}\left[\begin{array}{c}\zeta_{l,\kappa}^{[1]}\,\mathbf{\Delta}_{\hbar}^{(a(w_1,w_2),q)}\mathcal{B}_t\left(a\left(w_1,w_2\right),1+\frac{\hbar-q}{\zeta_1}\right)\\ -\zeta_{l,\kappa}^{[2]}\,\mathbf{\Delta}_{\hbar}^{(1+a(w_1,w_2),q)}\mathcal{B}_t\left(1+a\left(w_1,w_2\right),1+\frac{\hbar-q}{\zeta_1}\right)\end{array}\right].\tag{10}$$

The L-moments are analogous to the ordinary moments but can be estimated by linear combinations of order statistics. They exist whenever the mean of the distribution exists, even though some higher moments may not exist, and are relatively robust to the effects of outliers. Based upon the moments in equation (10), we can derive explicit expressions for the L-moments of Y as infinite weighted linear combinations of the means of suitable PTL-Lx order statistics. They are linear functions of expected order statistics defined by

$$\lambda_{r,Y} = \frac{1}{r}\sum_{d=0}^{r-1}(-1)^{d} E\left(Y_{r-d:r}\right)\binom{r-1}{d},\ r \geq 1.$$

3. copulas

3.1. BPTL-Lx type via FGM copula

Consider the joint CDF of the FGM family (Gumbel [35] and Gumbel [36]), then

$$C_{\boldsymbol{\Upsilon}\in(-1,1)}(d,w)|_{\boldsymbol{\Upsilon}\in(-1,1)} = dw\left(1+\boldsymbol{\Upsilon}\overline{d}\overline{w}\right),$$

where the marginal function $d = F_1(y_1)$, $w = F_2(y_2)$ is a dependence parameter and for every $d,w \in (0,1)^2$, $C_{\boldsymbol{\Upsilon}}(d,0) = C_{\boldsymbol{\Upsilon}}(0,w) = 0$ which is “grounded minimum” and $C_{\boldsymbol{\Upsilon}}(d,1) = d$ and $C_{\boldsymbol{\Upsilon}}(1,w) = w$ which is “grounded maximum”. Then, we have

$$\begin{aligned} F_{\boldsymbol{\Upsilon}}(y_1,y_2) \quad = \quad & \frac{1-\mathbf{g}_{b_1,a_1,\zeta_1,\zeta_2}\left(y_1\right)}{b_{*1}}\frac{1-\mathbf{g}_{b_2,a_2,\zeta_1,\zeta_2}\left(y_2\right)}{b_{*2}} \\ & \times\left(1+\boldsymbol{\Upsilon}\left[\overline{\mathbf{g}}_{b_1,a_1,\zeta_1,\zeta_2}\left(y_1\right)\overline{\mathbf{g}}_{b_2,a_2,\zeta_1,\zeta_2}\left(y_2\right)\right]\right). \end{aligned}$$

where

$$\mathbf{g}_{b_1,a_1,\zeta_1,\zeta_2}\left(y_1\right) = \exp\left\{-b_1\left[1-\left(1+\frac{y_1}{\zeta_2}\right)^{-2\zeta_1}\right]^{a_1}\right\},$$

$$\mathbf{g}_{b_2,a_2,\zeta_1,\zeta_2}\left(y_2\right) = \exp\left\{-b_2\left[1-\left(1+\frac{y_2}{\zeta_2}\right)^{-2\zeta_1}\right]^{a_2}\right\},$$

$$\overline{\mathbf{g}}_{b_1,a_1,\zeta_1,\zeta_2}\left(y_1\right) = 1-\mathbf{g}_{b_1,a_1,\zeta_1,\zeta_2}\left(y_1\right)$$

and

$$\overline{\mathbf{g}}_{b_2,a_2,\zeta_1,\zeta_2}\left(y_2\right) = 1-\mathbf{g}_{b_2,a_2,\zeta_1,\zeta_2}\left(y_2\right).$$

The joint PDF can then derived from

$$c_{\boldsymbol{\Upsilon}}(d,w) = 1+\boldsymbol{\Upsilon}d^{*}w^{*}|_{(d^{*}=1-2d \text{ and } w^{*}=1-2w)}.$$

3.2. BvOBGR type via modified FGM copula

Consider the following modified version of the bivariate FGM copula defined as (see Rodriguez-Lallena and Ubeda-Flores [46])

$$C_{\boldsymbol{\Upsilon}}(d,w)|_{\boldsymbol{\Upsilon}\in[-1,1]} = dw\left[1+\boldsymbol{\Upsilon}\wp\left(d\right)\psi\left(w\right)\right] = dw+\boldsymbol{\Upsilon}A\left(d\right)B\left(w\right),$$

where $A(d) = d\wp(d)$, and $B(w) = w\psi(w)$. Where $\wp(d)$ and $\psi(w)$ are two absolutely continuous functions on $(0,1)$ with the following conditions:

1-The boundary condition:

$$\wp\left(0\right) = \wp\left(1\right) = \psi\left(0\right) = \psi\left(1\right) = 0.$$

2-Let

$$\tau_1 = \inf\left\{\frac{\partial}{\partial d}A(d)\,|\Lambda_1(d)\right\} < 0,$$

$$\tau_2 = \sup\left\{\frac{\partial}{\partial d}A(d)\,|\Lambda_1(d)\right\} < 0,$$

$$\pi_1 = \inf\left\{\frac{\partial}{\partial w}B(w)\,|\Lambda_2(w)\right\} > 0,$$

$$\pi_2 = \sup\left\{\frac{\partial}{\partial w}B(w)\,|\Lambda_2(w)\right\} > 0,$$

Then, $\min(\tau_1\tau_2, \pi_1\pi_2) \geq 1$ where

$$\frac{\partial}{\partial d}A(d) = \wp(d) + d\frac{\partial}{\partial d}\wp(d),$$

$$\Lambda_1(d) = \left\{d : d \in (0,1)\,|\frac{\partial}{\partial d}A(d) \quad \text{exists}\right\},$$

and

$$\Lambda_2(w) = \left\{w : w \in (0,1)\,|\frac{\partial}{\partial w}B(w) \quad \text{exists}\right\}.$$

3.2.1. BPTL-Lx-FGM (Type I) model

Here, we consider the following functional form for both $A(d)$ and $B(w)$ as

$$C_{\mathbf{\Upsilon}}(y_1, y_2) = \frac{1 - \mathbf{g}_{b_1,a_1,\zeta_1,\zeta_2}(y_1)}{b_{*1}}\frac{1 - \mathbf{g}_{b_2,a_2,\zeta_1,\zeta_2}(y_2)}{b_{*2}} + \mathbf{\Upsilon}A(y_1)B(y_2)\;,$$

where

$$A(y_1) = \frac{1 - \mathbf{g}_{b_1,a_1,\zeta_1,\zeta_2}(y_1)}{b_{*1}}\overline{\mathbf{g}}_{b_1,a_1,\zeta_1,\zeta_2}(y_1)$$

and

$$B(y_2) = \frac{1 - \mathbf{g}_{b_2,a_2,\zeta_1,\zeta_2}(y_2)}{b_{*2}}\overline{\mathbf{g}}_{b_2,a_2,\zeta_1,\zeta_2}(y_2).$$

3.2.2. BPTL-Lx-FGM (Type II) model

Due to Ghosh and Ray [32] the CDF of the BPTL-Lx-FGM (Type II) model can be derived from

$$C_{\mathbf{\Upsilon}}(d, w) = \frac{1 - \mathbf{g}_{b_1,a_1,\zeta_1,\zeta_2}(d)}{b_{*1}}F^{-1}(w) + \frac{1 - \mathbf{g}_{b_2,a_2,\zeta_1,\zeta_2}(w)}{b_{*2}}F^{-1}(d) - F^{-1}(d)F^{-1}(w),$$

where

$$F^{-1}(d) = \zeta_2\left(\left\{1 - \left[-\frac{1}{b_1}\ln(1 - db_{*1})\right]^{\frac{1}{a_1}}\right\}^{-\frac{1}{2\zeta_1}} - 1\right),$$

and

$$F^{-1}(w) = \zeta_2\left(\left\{1 - \left[-\frac{1}{b_2}\ln(1 - wb_{*2})\right]^{\frac{1}{a_2}}\right\}^{-\frac{1}{2\zeta_1}} - 1\right).$$

3.2.3. BPTL-Lx-FGM (Type III) model

Consider the following functional form for both $A(d)|_{(\boldsymbol{\Upsilon}_1>0)} = d^{\boldsymbol{\Upsilon}_1}(1-d)^{1-\boldsymbol{\Upsilon}_1}$ and $Z(w)|_{(\boldsymbol{\Upsilon}_2>0)} = w^{\boldsymbol{\Upsilon}_2}(1-w)^{1-\boldsymbol{\Upsilon}_2}$ which satisfy all the conditions stated earlier. Then, the corresponding bivariate copula (henceforth, BPTL-Lx-FGM (Type III) copula) can be derived from

$$C_{\boldsymbol{\Upsilon},\boldsymbol{\Upsilon}_1,\boldsymbol{\Upsilon}_2}(d,w) = dw\left[1+\boldsymbol{\Upsilon}A(d)\,Z(w)\right].$$

Therefore

$$\begin{aligned} C_{\boldsymbol{\Upsilon},\boldsymbol{\Upsilon}_1,\boldsymbol{\Upsilon}_2}(d,w) &= \frac{1-\mathbf{g}_{b_1,a_1,\zeta_1,\zeta_2}(d)}{b_{*1}}\frac{1-\mathbf{g}_{b_2,a_2,\zeta_1,\zeta_2}(w)}{b_{*2}} \\ &\times\left(1+\boldsymbol{\Upsilon}\left\{\begin{array}{c} \left[\frac{1-\mathbf{g}_{b_1,a_1,\zeta_1,\zeta_2}(d)}{b_{*1}}\right]^{\boldsymbol{\Upsilon}_1}\overline{\mathbf{g}}^{1-\boldsymbol{\Upsilon}_1}_{b_1,a_1,\zeta_1,\zeta_2}(d) \\ \times\left[\frac{1-\mathbf{g}_{b_2,a_2,\zeta_1,\zeta_2}(w)}{b_{*2}}\right]^{\boldsymbol{\Upsilon}_2}\overline{\mathbf{g}}^{1-\boldsymbol{\Upsilon}_2}_{b_2,a_2,\zeta_1,\zeta_2}(w)\end{array}\right\}\right)\end{aligned}$$

3.2.4. BPTL-Lx-FGM (Type IV) model

Consider the following functional form for both $C(d) = d\log\left(1+\overline{d}\right)$ and $D(w) = w\log(1+\overline{w})$ which satisfy all the conditions stated earlier. In this case, one can also derive a closed form expression for the associated CDF of the BPTL-Lx-FGM (Type IV) as

$$C_{\boldsymbol{\Upsilon}}(d,w) = dw\left[1+\boldsymbol{\Upsilon}C(d)\,D(w)\right].$$

Hence

$$\begin{aligned} C_{\boldsymbol{\Upsilon}}(d,w) &= \frac{1-\mathbf{g}_{b_1,a_1,\zeta_1,\zeta_2}(d)}{b_{*1}}\frac{1-\mathbf{g}_{b_2,a_2,\zeta_1,\zeta_2}(w)}{b_{*2}} \\ &\times\left(1+\boldsymbol{\Upsilon}\left\{\begin{array}{c} d\log\left[1+\overline{\mathbf{g}}_{b_1,a_1,\zeta_1,\zeta_2}(d)\right] \\ \times w\log\left[1+\overline{\mathbf{g}}_{b_2,a_2,\zeta_1,\zeta_2}(w)\right]\end{array}\right\}\right)\end{aligned}$$

3.3. BPTL-Lx type via Renyi's entropy

Consider theorem of Pougaza and Djafari [45] where

$$C(d,w) = y_2 d + y_1 w - y_1 y_2,$$

where d and W are two absolutely continuous functions on $(0,1)$. Then, the associated BPTL-Lx will be

$$C(y_1,y_2) = \frac{1-\mathbf{g}_{b_1,a_1,\zeta_1,\zeta_2}(y_1)}{b_{*1}}y_2 + \frac{1-\mathbf{g}_{b_2,a_2,\zeta_1,\zeta_2}(y_2)}{b_{*2}}y_1 - y_1 y_2.$$

3.4. BPTL-Lx type via Clayton copula

The Clayton copula can be considered as

$$C_{\boldsymbol{\Upsilon}}(w_1,w_2) = \left(w_1^{-\boldsymbol{\Upsilon}} + w_2^{-\boldsymbol{\Upsilon}} - 1\right)^{-\frac{1}{\boldsymbol{\Upsilon}}}|_{\boldsymbol{\Upsilon}\in[0,\infty]}.$$

Let us assume that $Y \sim$PTL-Lx $(\underline{\boldsymbol{\Theta}}_1)$ and $Z \sim$PTL-Lx $(\underline{\boldsymbol{\Theta}}_2)$. Then, setting

$$w_1 = w\left(y|\underline{\boldsymbol{\Theta}}_1\right) = \frac{1}{b_{*1}}\left[1-\mathbf{g}_{b_1,a_1,\zeta_1,\zeta_2}(w_1)\right],$$

and

$$w_2 = w\left(z|\underline{\boldsymbol{\Theta}}_2\right) = \frac{1}{b_{*2}}\left[1-\mathbf{g}_{b_2,a_2,\zeta_1,\zeta_2}(w_2)\right].$$

Then, the BPTL-Lx type distribution can be derived as

$$F_{\boldsymbol{\Upsilon}}(y,z)=C_{\boldsymbol{\Upsilon}}\left(F_{\underline{\boldsymbol{\Theta}}_1}(y),F_{\underline{\boldsymbol{\Theta}}_2}(z)\right)=\left\{\begin{array}{c}\left[\frac{1-\mathbf{g}_{b_1,a_1,\zeta_1,\zeta_2}(w_1)}{b_{*1}}\right]^{-\boldsymbol{\Upsilon}}\\+\left[\frac{1-\mathbf{g}_{b_2,a_2,\zeta_1,\zeta_2}(w_2)}{b_{*2}}\right]^{-\boldsymbol{\Upsilon}}-1\end{array}\right\}^{-\frac{1}{\boldsymbol{\Upsilon}}}.$$

3.5. MPTL-Lx extention via Clayton copula

A straightforward n-dimensional extension from the above will be

$$C(w_i)=\left(\sum_{i=1}^{n}w_i^{\boldsymbol{\Upsilon}}+1-n\right)^{-\frac{1}{\boldsymbol{\Upsilon}}}.$$

Then, the MPTL-Lx extention can expressed as

$$C(\underline{Z})=\left(\sum_{i=1}^{n}\left\{\frac{1-\mathbf{g}_{b_i,a_i,\zeta_1,\zeta_2}(w_i)}{b_{*i}}\right\}^{-\boldsymbol{\Upsilon}}+1-n\right)^{-\frac{1}{\boldsymbol{\Upsilon}}},$$

where $\underline{Z}=z_1,z_2,\cdots,z_n$. For more details see Ali et al. [3], Ali et al. [4], Elgohari and Yousof [20], Elgohari and Yousof [21], Elgohari and Yousof [22], Elgohari et al. [23], Shehata and Yousof [49], Al-Babtain et al. [1], Al-Babtain et al. [2], Salah et al. [47], Shehata et al. [50], Shehata and Yousof [48] and Yousof et al. [60].

4. Graphical assessment

Graphically and using the biases and mean squared errors (MSEs), we can perform the simulation experiments to assess the finite sample behavior of the maximum likelihood estimations (MLEs). The assessment was based on N=1000 replication for all $n|_{(n=50,100,\ldots,500)}$. The following algorithm is considered:

1. Generate N=1000 samples of size $n|_{(n=50,100,\ldots,500)}$ from the PTL-Lx distribution using (4);

$$y_u=\zeta_2\left(\left(\left\{1-\left[-\frac{1}{b}\ln\left(1-ub_*\right)\right]^{\frac{1}{a}}\right\}^{-\frac{1}{2\zeta_1}}-1\right)\right).$$

2. Compute the MLEs for the N=1000 samples, say

$$\left(\widehat{a_n},\widehat{b_n},\widehat{\zeta_{1n}},\widehat{\zeta_{2n}}\right)|_{(n=1,2,\ldots,1000)},$$

3. Compute the SEs of the MLEs for the 1000 samples, say

$$\left(\kappa_{\widehat{a_n}},\kappa_{\widehat{b_n}},\kappa_{\widehat{\zeta_{1n}}},\kappa_{\widehat{\zeta_{2n}}}\right)|_{(n=1,2,\ldots,1000)}.$$

The standard errors (SEs) were computed by inverting the observed information matrix.

4. Compute the biases and mean squared errors given for $\underline{\boldsymbol{\Theta}}=a,b,\zeta_1,\zeta_2$. We repeated these steps for $n|_{(n=50,100,\ldots,500)}$ with $b=1,2,..,100,a=1,2,..,100,\ \zeta_1=1,2,..,100,\ \zeta_2=1,2,..,100$, so computing biases$\left(\text{Bias}_{\underline{\boldsymbol{\Theta}}}(n)\right)$, mean squared errors (MSEs) $\left(MSE_h(n)\right)$ for $\underline{\boldsymbol{\Theta}}=a,b,\zeta_1,\zeta_2$ and $n|_{(n=50,100,\ldots,500)}$ where

$$\text{Bias}_{\underline{\boldsymbol{\Theta}}}(n)|_{(\underline{\boldsymbol{\Theta}}=a,b,\zeta_1,\zeta_2)}=\frac{1}{1000}\sum_{n=1}^{1000}\left(\widehat{\underline{\boldsymbol{\Theta}}}_n-\underline{\boldsymbol{\Theta}}\right),$$

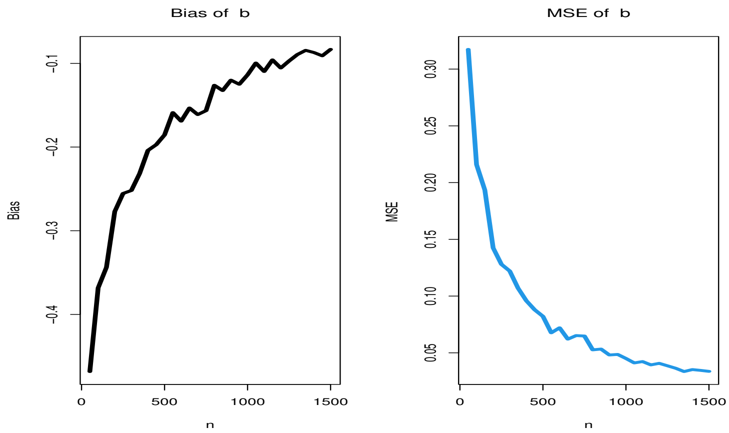

Figure 2. biases and mean squared errors for the parameter a.

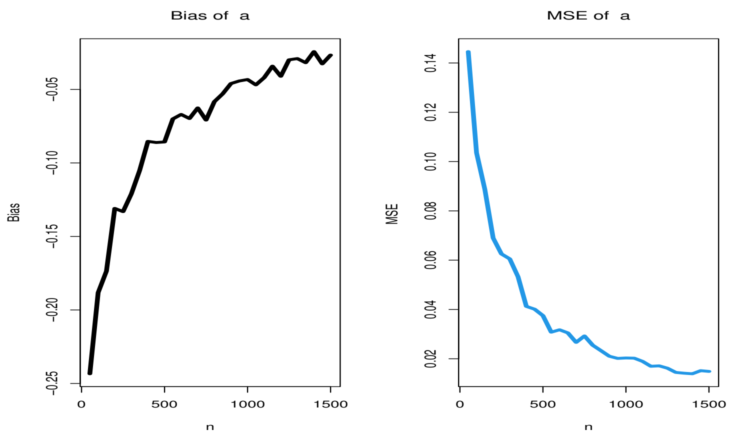

Figure 3. biases and mean squared errors for the parameter b.

and

$$MSE_{\underline{\mathbf{\Theta}}}(n)|_{(\underline{\mathbf{\Theta}}=a,b,\zeta_1,\zeta_2)} = \frac{1}{1000}\sum_{n=1}^{1000}\left(\widehat{\underline{\mathbf{\Theta}}}_n - \underline{\mathbf{\Theta}}\right)^2.$$

Figure 2, Figure 3, Figure 4 and Figure 5 give the biases (left panels) and MSEs (right panels) for the parameters a, b, ζ_1 and ζ_2 respectively. The left panels from show how the four biases vary with respect to n. The right panels show how the four MSEs vary with respect to n. The broken line in red in Figure 6 corresponds to the biases being 0. From Figure 2, Figure 3, Figure 4 and Figure 5 (left panels), the biases for each parameter are generally negative and tends to zero as $n \to \infty$. From Figure 2, Figure 3, Figure 4 and Figure 5 (right panels), the MSEs for each parameter decrease to zero as $n \to \infty$.

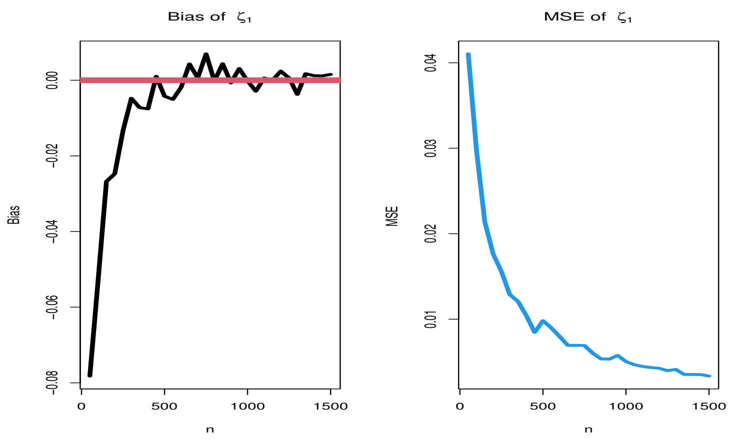

Figure 4. biases and mean squared errors for the parameter ζ_1.

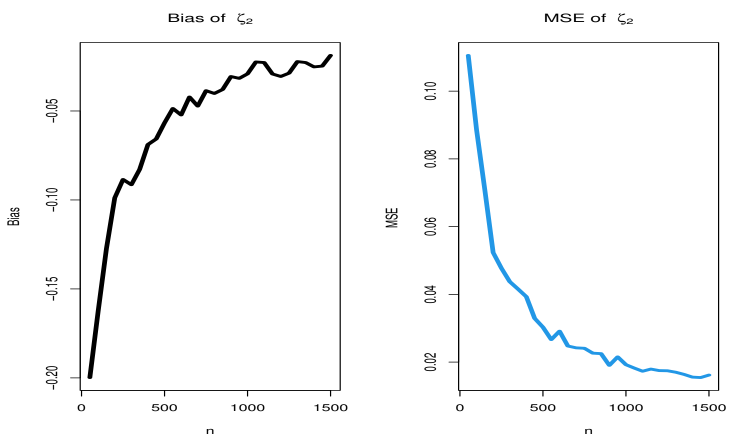

Figure 5. biases and mean squared errors for the parameter ζ_2.

5. Applications

In this section, we provide two real life applications to two real data sets to illustrate the importance and flexibility of the PTL-Lx model. We compare the fit of the PTL-Lx with some well-known competitive models (see Table 2).

Table 2: The competitive models.

N.	Model	Abbreviation
1	Lomax (two paramters)	Lx
2	Exponentiated Lx (three paramters)	Exp-Lx
3	Kumaraswamy Lx (four paramters)	K-Lx
4	Macdonald Lx (four paramters)	Mc-Lx
5	Beta Lx (four paramters)	B-Lx
6	Gamma Lx (four paramters)	Ga-Lx
7	Transmuted Topp-Leone Lx (four paramters)	TTL-Lx
8	Reduced TTL-Lx (three paramters)	RTTL-Lx
9	Odd log-logistic Lx (three paramters)	OLL-Lx
10	Reduced OLL-Lx (wo paramters)	ROLL-Lx
11	Reduced Burr-Hatke Lx (two paramters)	RBH-Lx
12	Special generalized mixture Lomax (three paramters)	SGM-Lx
13	Reduced PTL-Lx (three paramters)	RPTL-Lx
14	Proportional reversed hazard rate Lx (three paramters)	PRHR-Lx

First data set: Failure times of 84 Aircraft Windshield: The first real data set (data set I) represents the data on failure times of 84 aircraft windshield given in Murthy et al. [44]. The data are: 0.0400, 1.866, 2.3850, 3.443, 0.3010, 1.876, 2.4810, 3.467, 0.309, 1.8990, 2.610, 3.4780, 0.557, 1.9110, 2.625, 3.5780, 0.943, 1.9120, 2.632, 3.5950, 1.0700, 1.914, 2.6460, 3.699, 1.1240, 1.981, 2.661, 3.7790,1.248, 2.0100, 2.688, 3.9240, 1.2810, 2.038, 2.820, 3, 4.035, 1.281, 2.0850, 2.890, 4.121, 1.3030, 2.089, 2.902, 4.167, 1.4320, 2.097, 2.934, 4.2400, 1.480, 2.135, 2.962, 4.2550, 1.505, 2.154, 2.9640, 4.278, 1.506, 2.190, 3.000, 4.3050, 1.568, 2.1940, 3.103, 4.376, 1.615, 2.2230, 3.114, 4.449, 1.6190, 2.224, 3.1170, 4.485, 1.652, 2.2290, 3.166, 4.570, 1.652, 2.3000, 3.344, 4.602, 1.7570, 2.324, 3.3760, 4.663.

Second data set: Service times of 63 Aircraft Windshield: The second real data set (data set II) represents the data on service times of 63 aircraft windshield given in Murthy et al. [44]. The data are: 0.046, 1.436, 2.592, 0.140, 1.492, 2.600, 0.150, 1.580, 2.670, 0.248, 1.7190, 2.717, 0.2800, 1.794, 2.819, 0.3130, 1.915, 2.820, 0.389, 1.9200, 2.878, 0.487, 1.9630, 2.950, 0.622, 1.978, 3.0030, 0.9000, 2.053, 3.1020, 0.952, 2.065, 3.3040, 0.9960, 2.117, 3.483, 1.0030, 2.137, 3.500, 1.0100, 2.141, 3.6220, 1.085, 2.163, 3.6650, 1.092, 2.183, 3.695, 1.1520, 2.2400, 4.015, 1.183, 2.3410, 4.628, 1.2440, 2.435, 4.806, 1.249, 2.4640, 4.881, 1.262, 2.5430, 5.140. Many other useful real life data sets can be found in Aryal et al. [8], Yousof et al. [61], Mansour et al. [41], Goual et al. [34] and Cordeiro et al. [14]. For exploring the extreme vaues, the box plot is plotted (see Figure 6). Based on Figure 6, we note that no extreme values were found in the two real life data sets. For checking the normality, the Quantile-Quantile (Q-Q) plot is sketched (see Figure 7). Based on Figure 7, we note that the normality is nearly exists. For exploring the HRF for real data, the total time test (TTT) plot is provided (see Figure 8). Based on Figure 8, we note that the HRF is “monotonically increasing” for the two real life data sets. For exploring the initial shape of real data nonparametrically, kernel density estimation (KDE) is provided (see Figure 9). Figure 9 show nonparametric KDE for exploring the data. Figure 10 and Figure 11 give the Probability-Probability (P-P) plot (top left), estemated PDF (EPDF) (top right), estemated CDF (ECDF) (bottom left) and estemated HRF (EHRF) (bottom right) for data set I and II respectively.

We estimate the unknown parameters of each model by maximum likelihood using “L-BFGS-B” method and the goodness-of-fit statistics Akaike information criterion (AIC), Bayesian IC (BIC) and Consistent AIC (CAIC) are used to compare the models. In general, the smaller the values of these statistics, the better the fit to the data. The required computations are obtained by using the “maxLik” and “goftest” sub-routines in R-software. For failure times data: the analysis results of are listed in Tables 3 and 4. Table 3 gives the MLEs and standard errors (SEs) for failure times data. Table 4 gives the $-\hat{\ell}$ and goodness-of-fits statistics for failure times data. For service times data: the analysis results of are listed in Tables 5 and 6. Table 5 gives the MLEs and SEs for service times data. Table 6 give the $-\hat{\ell}$ and goodness-of-fits statistics for the service times data. Based on Tables 4 and 6, we note that

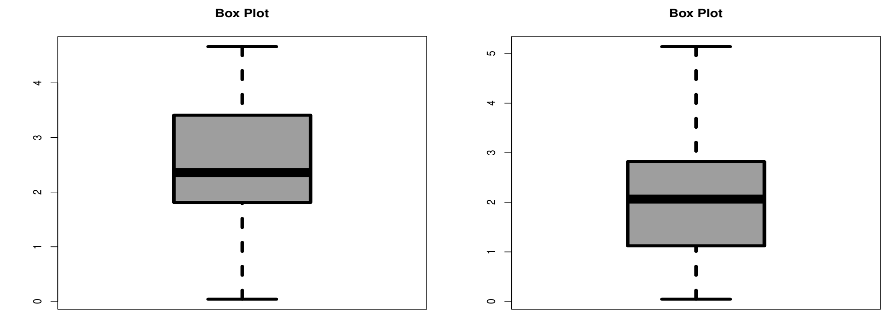

Figure 6. Box plots.

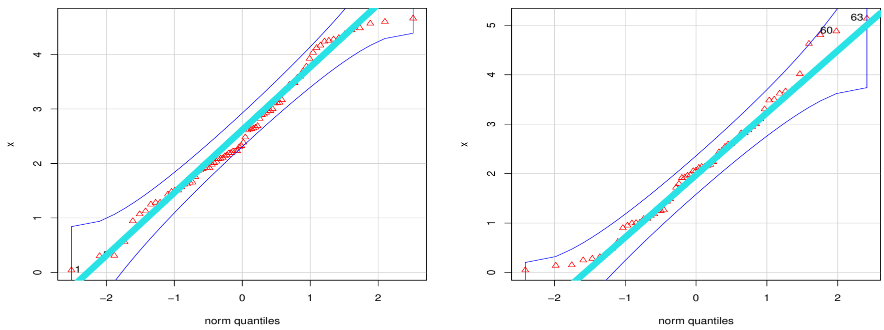

Figure 7. Q-Q plots.

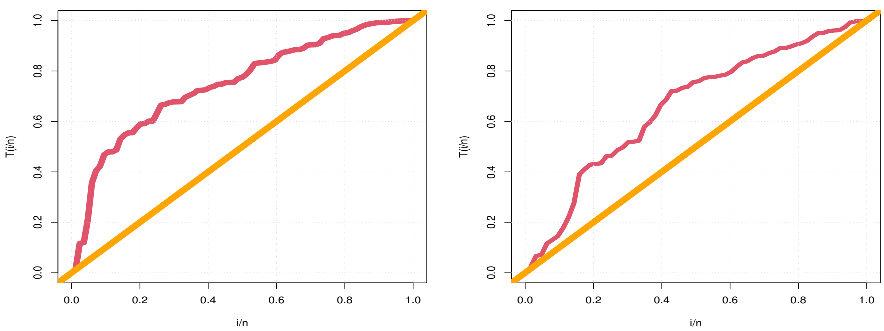

Figure 8. TTT plots.

the PTL-Lx model gives the lowest values for the AIC, CAIC, BIC and HQIC among all fitted models. Hence, it could be chosen as the best model under these criteria.

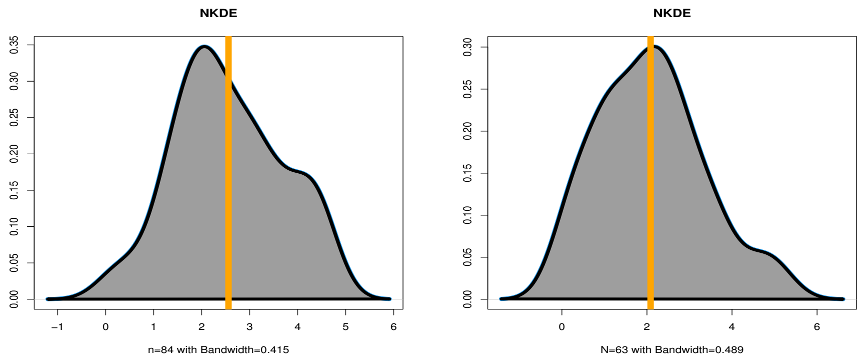

Figure 9. KDE plots.

Table 3: MLEs and SEs for failure times data.

Model	Estimates				
PTL-Lx(a,b,ζ_1,ζ_2)	-8.61942	0.38072	1511.814	4817.088	
	(6.22168)	(0.3761)	(292.445)	(548.812)	
Mc-Lx(a,b,c,ζ_1,ζ_2)	2.187521	119.1751	12.41714	19.92433	75.6606
	(0.5211)	(140.297)	(20.845)	(38.9601)	(147.24)
TTL-Lx(a,b,ζ_1,ζ_2)	-0.80750	2.47663	(15608.2)	(38628.3)	
	(0.13960)	(0.54176)	(1602.37)	(123.936)	
K-Lx(a,b,ζ_1,ζ_2)	2.6150	100.2756	5.27710	78.6774	
	(0.3822)	(120.486)	(9.8116)	(186.005)	
B-Lx(a,b,ζ_1,ζ_2)	3.60360	33.63870	4.830700	118.8374	
	(0.6187)	(63.7145)	(9.23820)	(428.927)	
PRHR-Lx(a,ζ_1,ζ_2)	3.73×10^6	4.707×10^{-1}	4.49×10^6		
	1.01×10^6	(0.00001)	37.14684		
RTTL-Lx(a,b,ζ_1)	-0.84732	5.52057	1.15678		
	(0.10010)	(1.18479)	(0.09588)		
SGM-Lx(b,ζ_1,ζ_2)	-1.04×10^{-1}	9.83×10^6	1.18×10^7		
	(0.1223)	(4843.3)	(501.04)		
OLL-Lx(b,ζ_1,ζ_2)	2.32636	(7.17×10^5)	$2.34\times10^6)$		
	(2.14×10^{-1})	(1.19×10^4)	(2.61×10^1)		
Ga-Lx(b,ζ_1,ζ_2)	3.58760	52001.49	37029.66		
	(0.5133)	(7955.00)	(81.1644)		
Exp-Lx(b,ζ_1,ζ_2)	3.62610	20074.51	26257.68		
	(0.6236)	(2041.83)	(99.7417)		
ROLL-Lx(b,ζ_1)	3.890564	0.57316			
	(0.36524)	(0.01946)			
RBH-Lx(ζ_1,ζ_2)	10801754	51367189			
	(983309)	(232312)			
Lx(ζ_1,ζ_2)	51425.35	131789.8			
	(5933.49)	(296.119)			

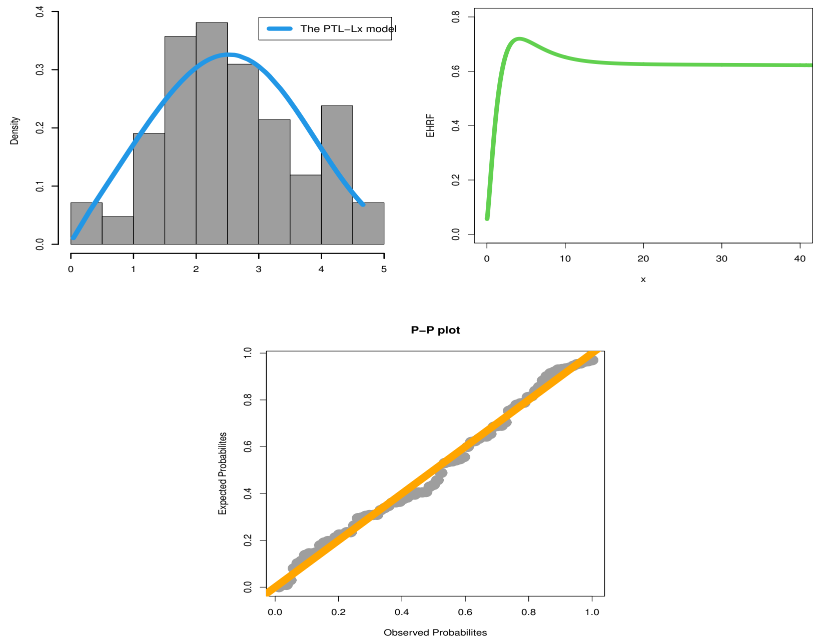

Figure 10. EPDF, EHRF and P-P plot for data set **I**.

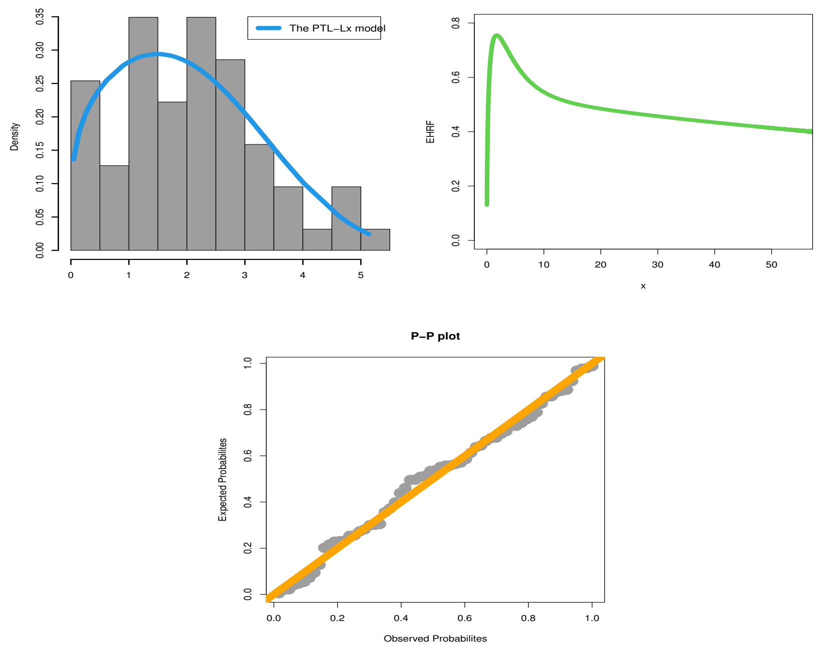

Figure 11. EPDF, EHRF and P-P plot for data set **I**.

Table 4: $-\hat{\ell}$ and goodness-of-fits statistics for failure times data.

Model	$-\hat{\ell}$	AIC	CAIC	BIC	HQIC
PTL-Lx	**107.2758**	**222.5516**	**223.058**	**232.2749**	**226.4603**
Mc-Lx	129.8023	269.6045	270.3640	281.8178	274.5170
RPTL-Lx	132.1993	270.3987	270.6987	277.6911	273.3302
OLL-Lx	134.4235	274.8470	275.1470	282.1394	277.7785
TTL-Lx	135.5700	279.1400	279.6464	288.8633	283.0487
Ga-Lx	138.4042	282.8083	283.1046	290.1363	285.7559
B-Lx	138.7177	285.4354	285.9354	295.2060	289.3654
Exp-Lx	141.3997	288.7994	289.0957	296.1273	291.7469
ROLL-Lx	142.8452	289.6904	289.8385	294.5520	291.6447
SGM-Lx	143.0874	292.1747	292.4747	299.4672	295.1062
PRHR-Lx	162.8770	331.7540	332.0540	339.0464	334.6855
Lx	164.9884	333.9767	334.1230	338.8620	335.9417
RBH-Lx	168.6040	341.2081	341.3562	346.0697	343.1624

Table 5: MLEs and SEs for service times data.

Model	Estimates			
PTL-Lx(a, b, ζ_1, ζ_2)	-138.3583	0.010947	43.9167	162.301
	(1.01027)	(7.96×10^{-3})	(7.0164)	(2.5831)
K-Lx(a, b, ζ_1, ζ_2)	1.66914	60.5673	2.56490	65.0640
	(0.2570)	(86.0131)	(4.7589)	(177.59)
B-Lx(a, b, ζ_1, ζ_2)	1.92183	31.2594	4.9684	169.5719
	(0.3184)	(316.841)	(50.528)	(339.207)
TTL-Lx(a, b, ζ_1, ζ_2)	(-0.6070)	1.785780	2123.391	4822.789
	(0.21371)	(0.41522)	(163.915)	(200.009)
PRHR-Lx(a, ζ_1, ζ_2)	1.59×10^{6}	3.93×10^{-1}	1.30×10^{6}	
	2.01×10^{3}	0.0004×10^{-1}	0.95×10^{6}	
RTTL-Lx(a, b, ζ_1)	-0.67145	2.74496	1.01238	
	(0.18746)	(0.6696)	(0.11405)	
SGM-Lx(b, ζ_1, ζ_2)	-1.04×10^{-1}	6.45×10^{6}	6.33×10^{6}	
	(4.1×10^{-10})	(3.21×10^{6})	(3.8573)	
OLL-Lx(b, ζ_1, ζ_2)	1.66419	6.340×10^{5}	2.01×10^{6}	
	(1.79×10^{-1})	(1.68×10^{4})	7.22×10^{6}	
Ga-Lx(b, ζ_1, ζ_2)	1.9073	35842.433	39197.57	
	(0.3213)	(6945.074)	(151.653)	
Exp-Lx(b, ζ_1, ζ_2)	1.9145	22971.154	32881.99	
	(0.3482)	(3209.533)	(162.230)	
ROLL-Lx(b, ζ_1)	2.37233	0.69109		
	(0.26825)	(0.04488)		
RBH-Lx(ζ_1, ζ_2)	14055522	53203423		
	(422.005)	(28.52323)		
Lx(ζ_1, ζ_2)	99269.78	207019.37		
	(11863.5)	(301.2366)		

Table 6: $-\hat{\ell}$ and goodness-of-fits statistics for the service times data.

Model	$-\hat{\ell}$	AIC	CAIC	BIC	HQIC
PTL-Lx	**75.96769**	**159.9354**	**160.625**	**168.5079**	**163.307**
K-Lx	100.8676	209.7353	210.4249	218.3078	213.1069
TTL-Lx	102.4498	212.8996	213.5893	221.4722	216.2713
Ga-Lx	102.8332	211.6663	212.0730	218.0958	214.1951
SGM-Lx	102.8940	211.7881	212.1949	218.2175	214.3168
B-Lx	102.9611	213.9223	214.6119	222.4948	217.2939
Exp-Lx	103.5498	213.0995	213.5063	219.5289	215.6282
OLL-Lx	104.9041	215.8082	216.2150	222.2376	218.3369
PRHR-Lx	109.2986	224.5973	225.004	231.0267	227.1264
Lx	109.2988	222.5976	222.7976	226.8839	224.2834
ROLL-Lx	110.7287	225.4573	225.6573	229.7436	227.1431
RTTL-Lx	112.1855	230.3710	230.7778	236.8004	232.8997
RBH-Lx	112.6005	229.2011	229.4011	233.4873	230.8869

6. Conclusions

A new four parameter compound lifetime model called the Poisson Topp-Leone Lomax (PTL-Lx) is defined and studied. The novel model is established based on the Poisson Topp-Leone family of Merovci et al. [43]. The PTL-Lx density function can be "right skewedwith heavy tail", "symmetric" and "left skewedwith heavy tail". The corresponding failure rate can be "monotonically decreasing", "increasing-constant", "upside down", "upside down-constant" and "reversed J-shape". The new PTL-Lx density can be expressed as as a mixture of the exponentiated Lomax densitied. The skewness of the PTL-Lx distribution can be positive. The spread for the kurtosis of the PTL-Lx model is ranging from -361.2494 to ∞. The index of dispersion for the PTL-Lx model can be in $(0, 1)$ and also > 1 so it may be used as an "under-dispersed" and "over-dispersed" model.

Relevant characteristics are derived and discussed. numerical and graphical analysis for some statistical properties are presented. we derived some new bivariate extensions via some common copulas such as Farlie Gumbel Morgenstern copula, modified Farlie Gumbel Morgenstern copula, Renyi's entropy and Clayton copula. The maximum likelihood method is used to estimate the PTL-Lx parameters. By means of "biases" and "mean squared errors", we performed simulation experiments to assess the finite sample behavior of the maximum likelihood estimators. It is noted that, the biases for all parameters are generally negative and tends to 0 as $n \to \infty$ and the mean squared errors for all parameter decrease to 0 as $n \to \infty$. The new model deserved to be chosen as the best model among many well-know Lomax extension.

As a future work, we can apply many new useful goodness-of-fit tests for right censored validation such as the Nikulin-Rao-Robson goodness-of-fit test, modified Nikulin-Rao-Robson goodness-of-fit test, Bagdonavicius-Nikulin goodness-of-fit test, modified Bagdonavicius-Nikulin goodness-of-fit test, to the new PTL-Lx model as performed by Ibrahim et al. [14], Mansour et al. ([41], [37], [38], [39], [40], [42]), Yadav et al. (2020), Ibrahim et al. [26], Yousof et al. [55], Yousof et al. [56], Yousof et al. [57], among others.

REFERENCES

1. Al-Babtain, A. A., Elbatal, I. and Yousof, H. M. (2020a). A new three parameter Fréchet model with mathematical properties and applications. Journal of Taibah University for Science, 14(1), 265-278.
2. Al-babtain, A. A., Elbatal, I. and Yousof, H. M. (2020b). A New Flexible Three-Parameter Model: Properties, Clayton Copula, and Modeling Real Data. Symmetry, 12(3), 440.

3. Ali, M. M., Yousof, H. M. and Ibrahim, M. (2021a). A new version of the generalized Rayleigh distribution with copula, properties, applications and different methods of estimation. Optimal Decision Making in Operations Research & Statistics: Methodologies and Applications, VOL 1, 1-25.
4. Ali, M. M., Ibrahim, M. and Yousof, H. M. (2021b). Expanding the Burr X model: properties, copula, real data modeling and different methods of estimation. Optimal Decision Making in Operations Research & Statistics: Methodologies and Applications, VOL 1, 26-49.
5. Atkinson, A. B. and Harrison, A. J. (1978). Distribution of Personal Wealth in Britain (Cambridge University Press, Cambridge).
6. Altun, E., Yousof, H. M. and Hamedani, G. G. (2018a). A new log-location regression model with influence diagnostics and residual analysis. Facta Universitatis, Series: Mathematics and Informatics, 33(3), 417-449.
7. Altun, E., Yousof, H. M., Chakraborty, S. and Handique, L. (2018b). Zografos-Balakrishnan Burr XII distribution: regression modeling and applications. International Journal of Mathematics and Statistics, 19(3), 46-70.
8. Aryal, G. R., Ortega, E. M., Hamedani, G. G. and Yousof, H. M. (2017). The Topp Leone Generated Weibull distribution: regression model, characterizations and applications, International Journal of Statistics and Probability, 6, 126-141.
9. Atkinson, A.B. and Harrison, A.J. (1978). Distribution of Personal Wealth in Britain (Cambridge University Press, Cambridge).
10. Balkema, A.A. and de Hann, L. Residual life at great age, Annals of Probability 2, 972–804, 1974.
11. Bryson, M. C. (1974). Heavy-tailed distribution: properties and tests, Technometrics 16, 161-68.
12. Chahkandi, M. and Ganjali, M. (2009). On some lifetime distributions with decrasing failure rate, Computational Statistics and Data Analysis 53, 4433–4440.
13. Chesneau, C. and Yousof, H. M. (2020). On a special generalized mixture class of probabilitic models. Journal of Nonlinear Modeling and Analysis, orthcoming.
14. Cordeiro, G. M., Yousof, H. M., Ramires, T. G. and Ortega, E. M. M. (2018). The Burr XII system of densities: properties, regression model and applications. Journal of Statistical Computation and Simulation, 88(3), 432-456.
15. Durbey, S. D. (1970). Compound gamma, beta and F distributions, Metrika 16, 27–31.
16. Gupta, R. C., Gupta, P. L. and Gupta, R. D. (1998). Modeling failure time data by Lehman alternatives. Communications in Statistics-Theory and methods, 27(4), 887-904.
17. Corbellini, A., Crosato, L., Ganugi, P and Mazzoli, M. (2007). Fitting Pareto II distributions on firm size: Statistical methodology and economic puzzles. Paper presented at the International Conference on Applied Stochastic Models and Data Analysis, Chania, Crete.
18. Cordeiro, G. M., Ortega, E. M. and Popovic, B. V. (2015). The gamma-Lomax distribution. Journal of Statistical computation and Simulation, 85(2), 305-319.
19. Elbiely, M. M. and Yousof, H. M. (2018). A New Extension of the Lomax Distribution and its Applications, Journal of Statistics and Applications, 2(1), 18-34.
20. Elgohari, H. and Yousof, H. M. (2020a). A Generalization of Lomax Distribution with Properties, Copula and Real Data Applications. Pakistan Journal of Statistics and Operation Research, 16(4), 697-711.
21. Elgohari, H. and Yousof, H. M. (2020b). New Extension of Weibull Distribution: Copula, Mathematical Properties and Data Modeling. Statistics, Optimization & Information Computing, 8(4), 972-993.
22. Elgohari, H. and Yousof, H. M. (2021). A New Extreme Value Model with Different Copula, Statistical Properties and Applications. Pakistan Journal of Statistics and Operation Research, 17(4), 1015-1035.
23. Elgohari, H., Ibrahim, M. and Yousof, H. M. (2021). A New Probability Distribution for Modeling Failure and Service Times: Properties, Copulas and Various Estimation Methods. Statistics, Optimization & Information Computing, 8(3), 555-586.
24. Harris, C.M. (1968). The Pareto distribution as a queue service descipline, Operations Research, 16, 307–313.
25. Hassan, A.S. and Al-Ghamdi, A.S. (2009). Optimum step stress accelerated life testing for Lomax distibution, Journal of Applied Sciences Research, 5, 2153–2164.
26. Ibrahim. M., Aidi, K., Ali, M. M. and Yousof, H. M. (2021). The Exponential Generalized Log-Logistic Model: Bagdonavičius-Nikulin test for Validation and Non-Bayesian Estimation Methods. Communications for Statistical Applications and Methods, forthcoming.
27. Ibrahim, M. and Yousof, H. M. (2020). A new generalized Lomax model: statistical properties and applications, Journal of Data Science, 18(1), 190 – 217.
28. Ibrahim, M., Yadav, A. S., Yousof, H. M., Goual, H. and Hamedani, G. G. (2019). A new extension of Lindley distribution: modified validation test, characterizations and different methods of estimation. Communications for Statistical Applications and Methods, 26(5), 473-495.
29. Lemonte, A. J. and Cordeiro, G. M. (2013). An extended Lomax distribution. Statistics, 47(4), 800-816.
30. Lomax, K.S. (1954). Business failures: Another example of the analysis of failure data, Journal of the American Statistical Association, 49, 847–852.
31. Gad, A. M., Hamedani, G. G., Salehabadi, S. M. and Yousof, H. M. (2019). The Burr XII-Burr XII distribution: mathematical properties and characterizations. Pakistan Journal of Statistics, 35(3), 229-248.
32. Ghosh, I. and Ray. S. (2016). Some alternative bivariate Kumaraswamy type distributions via copula with application in risk management. Journal of Statistical Theory and Practice 10, 693–706.
33. Goual, H. and Yousof, H. M. (2019). Validation of Burr XII inverse Rayleigh model via a modified chi-squared goodness-of-fit test. Journal of Applied Statistics, 47(1), 1-32.
34. Goual, H., Yousof, H. M. and Ali, M. M. (2020). Lomax inverse Weibull model: properties, applications and a modified Chi-squared goodness-of-fit test for validation, Journal of Nonlinear Science and Applications. 13(6), 330-353.
35. Gumbel, E. J. (1961). Bivariate logistic distributions. Journal of the American Statistical Association, 56(294), 335-349.
36. Gumbel, E. J. (1960) Bivariate exponential distributions. Journ. Amer. Statist. Assoc., 55, 698-707.
37. Mansour, M. M., Ibrahim, M., Aidi, K., Shafique Butt, N., Ali, M. M., Yousof, H. M. and Hamed, M. S. (2020a). ANew Log-Logistic Lifetime Model with Mathematical Properties, Copula, Modified Goodness-of-Fit Test for Validation and Real Data Modeling. Mathematics, 8(9), 1508.

38. Mansour, M. M., Butt, N. S., Ansari, S. I., Yousof, H. M., Ali, M. M. and Ibrahim, M. (2020b). A new exponentiated Weibull distribution's extension: copula, mathematical properties and applications. Contributions to Mathematics, 1 (2020) 57–66. DOI: 10.47443/cm.2020.0018
39. Mansour, M., Korkmaz, M. C., Ali, M. M., Yousof, H. M., Ansari, S. I. and Ibrahim, M. (2020c). A generalization of the exponentiated Weibull model with properties, Copula and application. Eurasian Bulletin of Mathematics, 3(2), 84-102.
40. Mansour, M., Rasekhi, M., Ibrahim, M., Aidi, K., Yousof, H. M. and Elrazik, E. A. (2020d). A New Parametric Life Distribution with Modified Bagdonavicius–Nikulin Goodness-of-Fit Test for Censored Validation, Properties, Applications, and Different Estimation Methods. Entropy, 22(5), 592.
41. Mansour, M., Yousof, H. M., Shehata, W. A. and Ibrahim, M. (2020e). A new two parameter Burr XII distribution: properties, copula, different estimation methods and modeling acute bone cancer data. Journal of Nonlinear Science and Applications, 13(5), 223-238.
42. Mansour, M. M., Butt, N. S., Yousof, H. M., Ansari, S. I. and Ibrahim, M. (2020f). A Generalization of Reciprocal Exponential Model: Clayton Copula, Statistical Properties and Modeling Skewed and Symmetric Real Data Sets. Pakistan Journal of Statistics and Operation Research, 16(2), 373-386.
43. Merovci, F., Yousof, H. M., & Hamedani, G. G. (2020). The Poisson Topp Leone Generator of Distributions for Lifetime Data: Theory, Characterizations and Applications. Pakistan Journal of Statistics and Operation Research, 16(2), 343-355.
44. Murthy, D.N.P. Xie, M. and Jiang, R. (2004). Weibull Models, Wiley.
45. Pougaza, D. B. and Djafari, M. A. (2011). Maximum entropies copulas. Proceedings of the 30th international workshop on Bayesian inference and maximum Entropy methods in Science and Engineering, 329-336.
46. Rodriguez-Lallena, J. A. and Ubeda-Flores, M. (2004). A new class of bivariate copulas. Statistics and Probability Letters, 66, 315–25.
47. Salah, M. M., El-Morshedy, M., Eliwa, M. S. and Yousof, H. M. (2020). Expanded Fréchet Model: Mathematical Properties, Copula, Different Estimation Methods, Applications and Validation Testing. Mathematics, 8(11), 1949.
48. Shehata, W. A. M. and Yousof, H. M. (2021a). A novel two-parameter Nadarajah-Haghighi extension: properties, copulas, modeling real data and different estimation methods. Statistics, Optimization & Information Computing, forthcoming.
49. Shehata, W. A. M. and Yousof, H. M. (2021b). The four-parameter exponentiated Weibull model with Copula, properties and real data modeling. Pakistan Journal of Statistics and Operation Research, 17(3), 649-667.
50. Shehata, W. A. M., Yousof, H. M. and Aboraya, M. (2021). A Novel Generator of Continuous Probability Distributions for the Asymmetric Left-skewed Bimodal Real-life Data with Properties and Copulas . Pakistan Journal of Statistics and Operation Research, 17(4), 943-961.
51. Tadikamalla, P. R. (1980). A look at the Burr and realted distributions, International Statistical Review 48, 337–344.
52. Yadav, A.S., Goual, H., Alotaibi, R.M. Rezk, H., Ali, M.M. and Yousof, H.M. (2020). Validation of the Topp-Leone-Lomax model via a modified Nikulin-Rao-Robson goodness-of-fit test with different methods of estimation. Symmetry, 12, 1-26. doi: 10.3390/sym12010057
53. Tahir, M. H., Cordeiro, G. M., Mansoor, M., & Zubair, M. (2015). The Weibull-Lomax distribution: properties and applications. Hacettepe Journal of Mathematics and Statistics, 44(2), 461-480.
54. Yousof, H. M., Ahsanullah, M. and Khalil, M. G. (2019). A New Zero-Truncated Version of the Poisson Burr XII Distribution: Characterizations and Properties. Journal of Statistical Theory and Applications, 18(1), 1-11.
55. Yousof, H. M., Aidi, K., Hamedani, G. G and Ibrahim, M. (2021). A new parametric lifetime distribution with modified Chi-square type test for right censored validation, characterizations and different estimation methods. Pakistan Journal of Statistics and Operation Research, 17(2), 399-425.
56. Yousof, H. M., Ali, M. M., Goual, H. and Ibrahim. M. (2021). A new reciprocal Rayleigh extension: properties, copulas, different methods of estimation and modified right censored test for validation, Statistics in Transition New Series, 23(3), 1-23.
57. Yousof, H. M., Al-nefaie, A. H., Aidi, K., Ali, M. M. and Ibrahim, M. (2021). A Modified Chi-square Type Test for Distributional Validity with Applications to Right Censored Reliability and Medical Data: A Modified Chi-square Type Test. Pakistan Journal of Statistics and Operation Research, 17(4), 1113-1121.
58. Yousof, H. M., Alizadeh, M., Jahanshahiand, S. M. A., Ramires, T. G., Ghosh, I. and Hamedani, G. G. (2017). The transmuted Topp-Leone G family of distributions: theory, characterizations and applications. Journal of Data Science, 15(4), 723-740.
59. Yousof, H. M., Altun, E., Ramires, T. G., Alizadeh, M. and Rasekhi, M. (2018). A new family of distributions with properties, regression models and applications, Journal of Statistics and Management Systems, 21, 1, 163-188.
60. Yousof, H. M., Hamedani, G. G. and Ibrahim, M. (2020). The Two-parameter Xgamma Fréchet Distribution: Characterizations, Copulas, Mathematical Properties and Different Classical Estimation Methods. Contributions to Mathematics, 2 (2020), 32-41.
61. Yousof, H. M., Majumder, M., Jahanshahi, S. M. A., Ali, M. M. and Hamedani G. G. (2018). A new Weibull class of distributions: theory, characterizations and applications, Journal of Statistical Research of Iran, 15, 45–83.